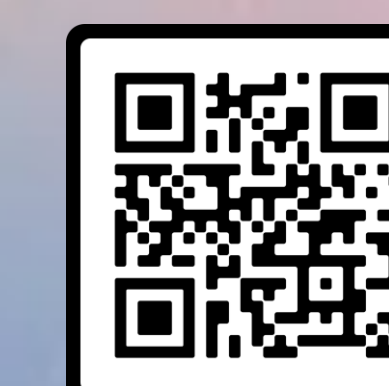


Do IHC results from single 2D histological sections reflect biomarker density in 3D tumor specimens in mouse tumor models?

Sepideh Mojtahedzadeh¹, Alan Opsahl¹, Dingzhou Li², Joan Aguilar¹, Timothy Coskran¹, Shawn P. O'Neil¹ and Sripad Ram^{1*}

¹Global Pathology and Investigative Toxicology, ²Drug Safety Statistics, Drug Safety R&D, Pfizer, Inc. *Corresponding author: Sripad.ram@Pfizer.com



SCAN ME



Abstract

Digital image analysis (DIA) of immunohistochemistry (IHC) assays is routinely performed to quantify immune cell infiltration in the tumor microenvironment for immuno-oncology projects. A retrospective analysis of our internal IHC-DIA data revealed significant variability in cell density estimates for nine immune cell biomarkers. To identify the sources of variability and to facilitate determination of group sizes in treatment arms, we performed a series of experiments to evaluate the distribution of cells expressing nine immune cell biomarkers in four different murine tumor models. By combining serial sectioning methods, IHC and whole-slide DIA, we investigated the extent of intra-tumor and inter-tumor variability for the nine immune cell biomarkers up to a depth of 1 mm in CT26, EMT6, KPC-ortho and KPC-GEM murine tumor models. Our analysis shows that inter-tumor variability is typically the dominant source of variation in immune cell density. Statistical power analysis revealed how group size and variance in immune cell density estimates affects the predictive power for detecting a statistically meaningful fold-change in immune cell density. Furthermore, the low level of intra-animal variability suggests that a single section from each tumor was adequate for estimating immune cell density for a given specimen. We anticipate that our results and analyses will provide guidelines for designing preclinical studies for immuno-oncology research and drug development.

Objectives

The objectives of the current study were to determine intra-animal and inter-animal variabilities in measurements of immune cell antigens localized by IHC and to estimate statistically relevant group sizes for treatment arms. We present a comprehensive analysis to quantify heterogeneity in the density of nine immune cell biomarkers (CD3, CD4, CD8a, CD11b, CD45, F4/80, FoxP3, GR1 and Granzyme B) at different depths in tumors collected from 4 murine tumor models (CT26, EMT6, KPC-ortho and KPC-GEM).

Materials and Methods

Materials

Species: Female BALB/c mice
Tumor models: CT26, EMT6, KPC Orthotopic (ortho), KPC genetically engineered mouse (GEM)
IHC antigens: CD3, CD4, CD8a, CD11b, CD45, F4/80, FoxP3, GR1, granzyme B (GZMB)

Histology:

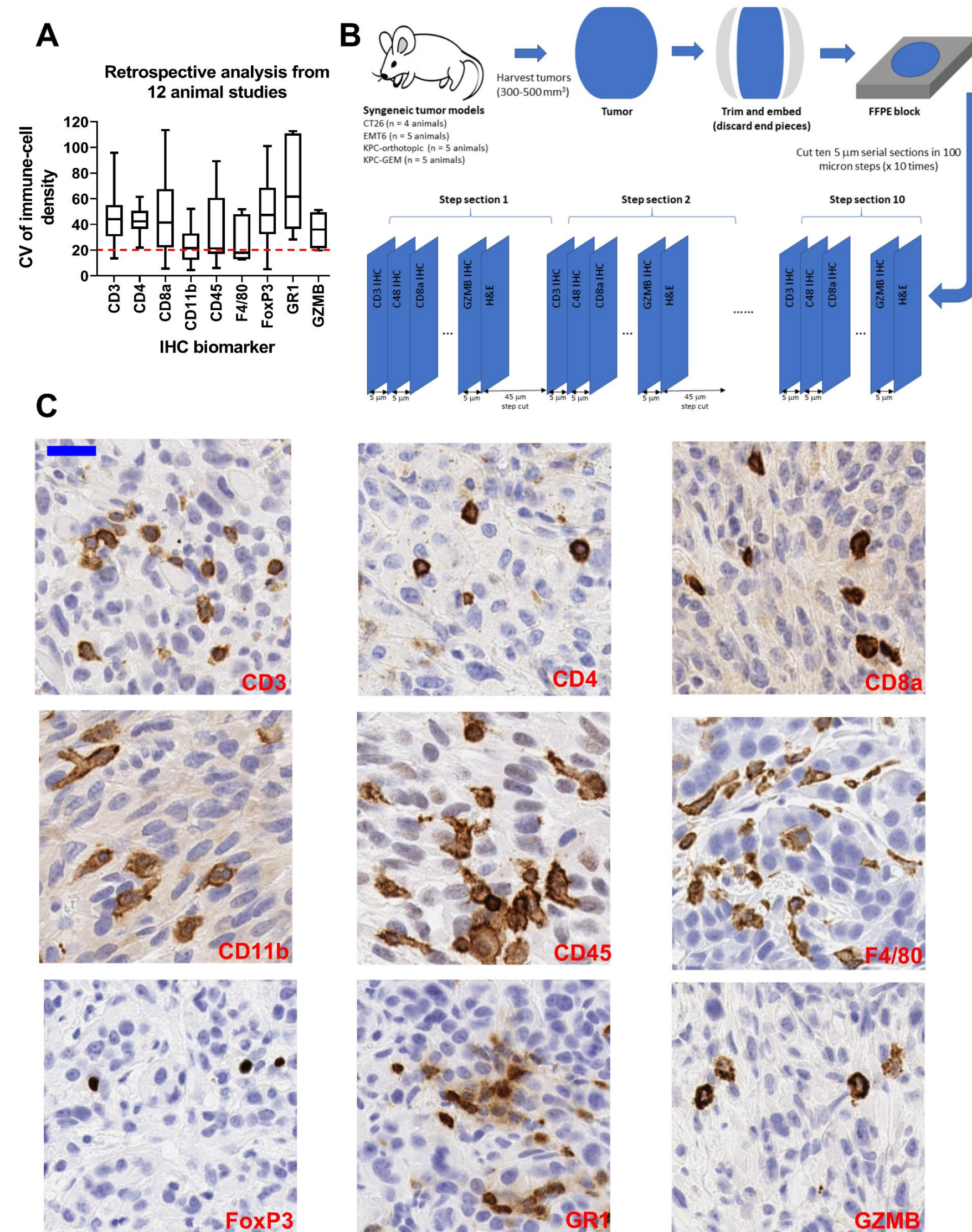


Figure 1. Retrospective analysis of animal-to-animal variability in immune cell density estimates.

Panel A shows the coefficient of variation (CV) of immune cell density estimates for nine biomarkers quantified through digital image analysis. The CV for each biomarker was calculated using data from the vehicle control groups taken from twelve different animal studies involving murine syngeneic tumor models. Panel B shows the study design to quantitatively assess intra-tumor and inter-tumor variability in four murine tumor models. Tumors were grown in mice, harvested, trimmed and archived as formalin-fixed, paraffin-embedded blocks. For each tumor sample, a set of ten serial sections (each 5 microns thick) were cut at 100-micron step intervals up to a depth of 1 mm. Each serial section at a given step was assigned to a biomarker and the order of assignment was maintained in all the steps. In this way, the abundance of each biomarker in the tumor tissue was sampled across ten sections that were each 100-microns apart and had similar tissue cross-sectional areas. Panel C shows representative regions cropped from IHC images of the immune cell biomarkers considered in this study. Here the biomarker of interest was immunolabeled and detected with the brown chromogen diaminobenzidine (DAB) and the sections were counter-stained with hematoxylin (blue) to label the nucleus. All images were cropped from whole-slide scans at 20x magnification. Scale bar equals 25 microns.

Image Analysis: All slides were scanned using an Aperio AT2 whole-slide digital scanner (Leica Biosystems, Vista, CA) at 20x magnification. Whole-slide, automated image analysis was performed using Visiopharm software. For each tumor model, custom apps were developed to detect the tissue in the image, to delineate viable tumor and non-tumor regions, and to compute the viable tumor area. In addition, areas of necrosis and hemorrhage identified on H&E images from serial sections were manually excluded from subsequent analysis. For each biomarker two custom apps were implemented, i.e., the cell count app and the stain area app. The cell count app detects and counts cells that are positive for the biomarker of interest in the viable tumor regions. The stain area app detects all pixels that are positive for the chromogen (DAB) used to label the biomarker of interest in the viable tumor regions and then outputs the total area of the positive pixels. The two DIA endpoints (i.e., immune cell density and stain area%) were quantified separately by different personnel in a semi-blinded manner.

Results

Intra-tumor and inter-tumor variability of immune cell biomarkers

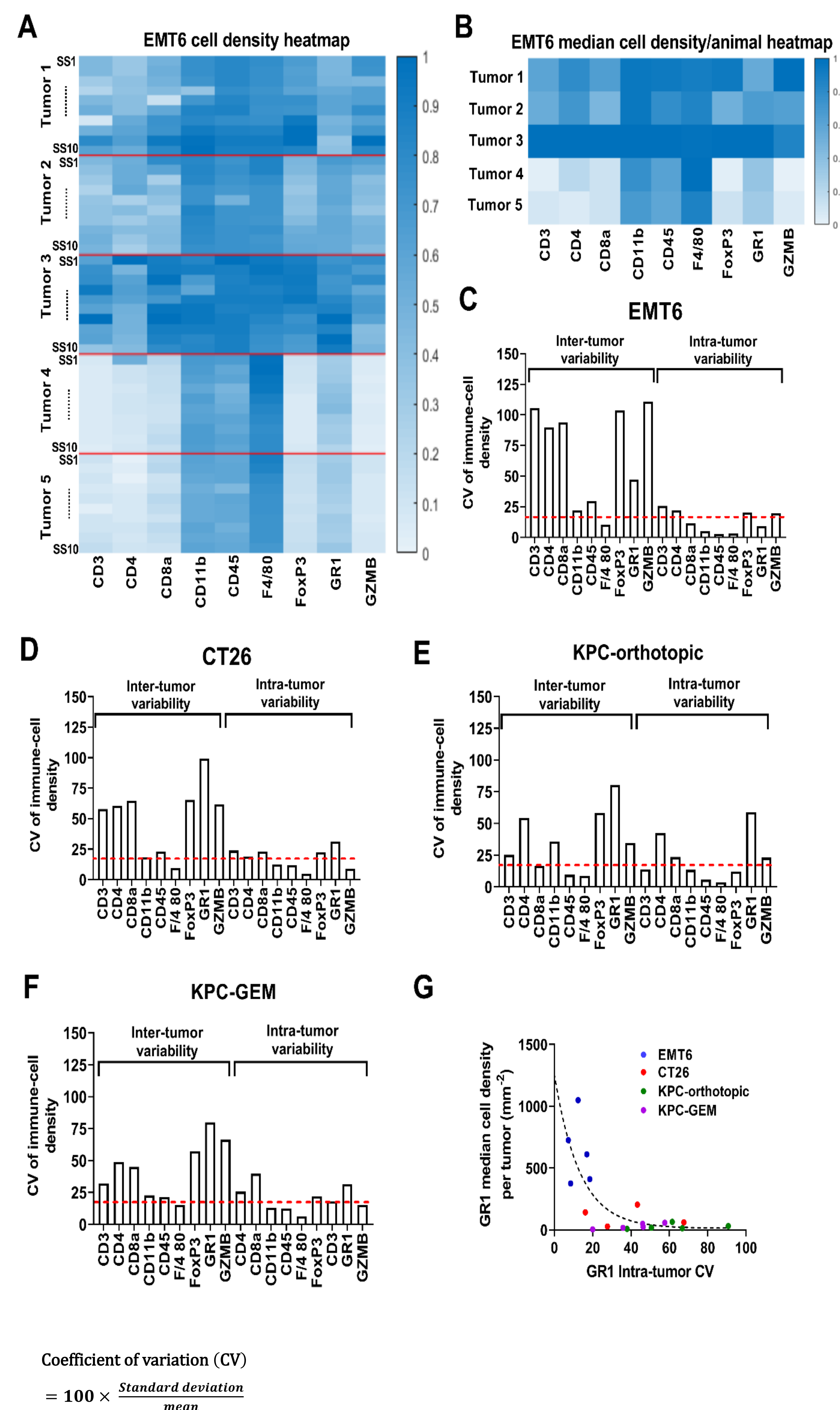


Figure 2. Intra-tumor and inter-tumor variability of immune cell abundance in syngeneic murine tumor models.

Panel A shows the heatmap of immune cell density estimates pertaining to the EMT6 tumor model for nine biomarkers across all step sections (SS) and animals. For display purposes, the immune cell density for each biomarker is normalized to 1 for all animals; thus, the results for all biomarkers can be compared using a global colormap. The heatmap color coding is comparable within tumor specimens for a given biomarker but not between biomarkers. Panel B shows the normalized heatmap of the median immune cell density for each biomarker for the EMT6 tumor model, calculated as the median of the ten step sections obtained from each animal. The heatmap is normalized in a manner that is analogous to the heatmap shown in Panel A. Panels C, D, E and F show the quantification of intra-tumor and inter-tumor variability for EMT6, CT26, KPC-orthotopic and KPC-GEM murine tumor models, respectively, for the nine immune cell biomarkers evaluated in this study. Panel G shows the plot of median cell density per animal versus intra-tumor CV for GR1 among different tumor models. An inverse relationship was observed between median cell density and the associated CV. Tumors with high cell density estimates tended to have lower intra-tumor CV, while tumors with low cell density estimates had higher intra-tumor CV.

Power Analysis

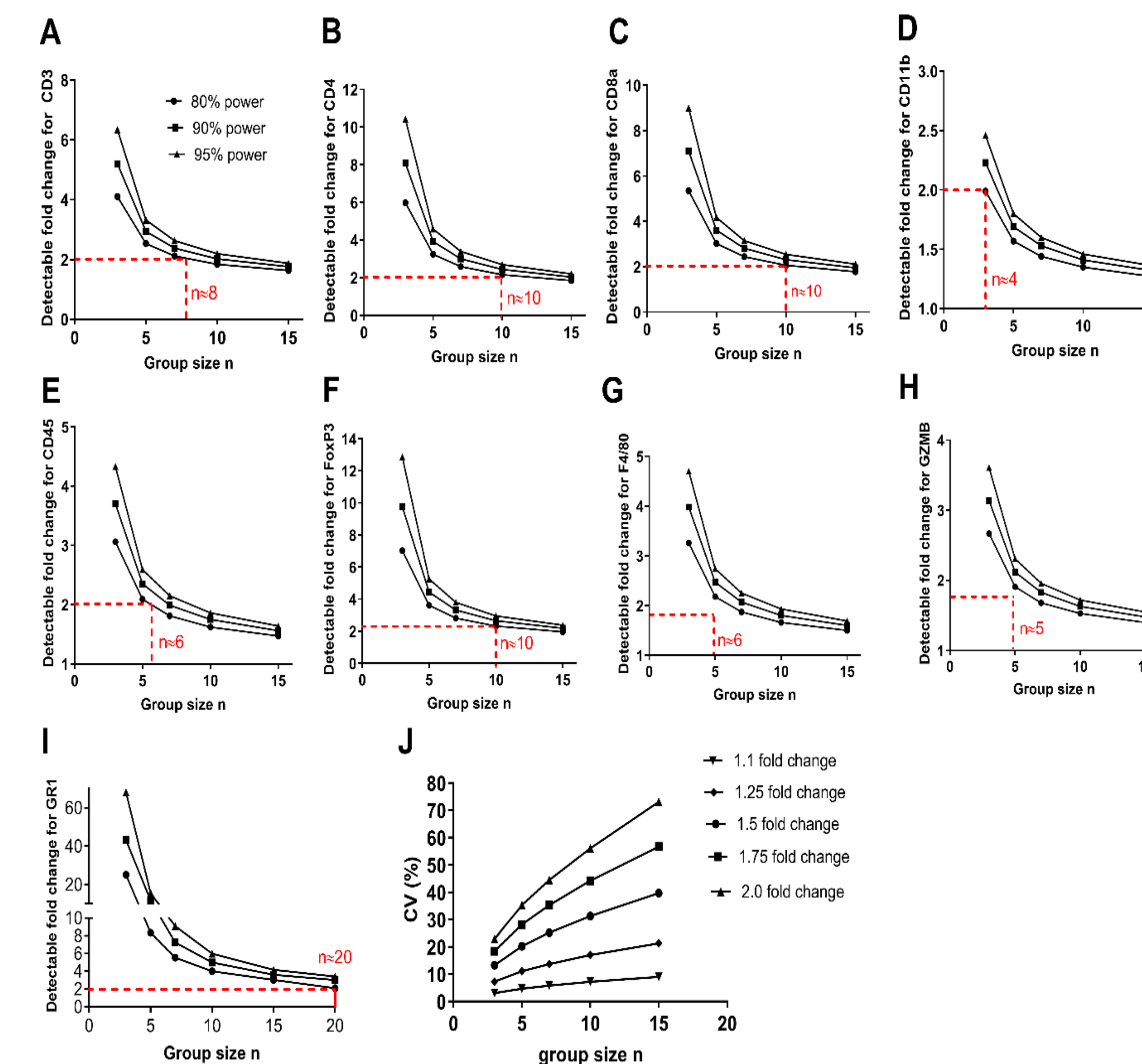


Figure 3. Results of statistical power analysis for IHC-DIA cell density estimates.

Panels A-I show the results of power analysis for different immune cell biomarkers to quantify the dependence of group size on statistically meaningful, detectable fold change in immune cell density estimates. For the power analysis calculations, the CV for each biomarker from the retrospective analysis (shown in Figure 1A) was considered at statistical power levels of 80%, 90% and 95%. The number of animals required to detect a 2-fold difference in cell density estimates at 80% power is indicated for each biomarker. Panel J shows the relationship between CV and group size for different fold-changes in cell density estimated at the 80% power level. The graph is complementary to the other panels in that it focuses on fold-change levels ranging from 1.1 to 2 and illustrates the relationship between CV of cell density and group size to detect a specific fold change.

Discussion

- This study provides a quantitative characterization of the variability in the density and proportion of immune cell infiltrates within and among tumor samples in four syngeneic tumor models. By using tumor models representing varying levels of complexity and translational relevance our results address longstanding questions concerning immunologic heterogeneity in murine tumors.
- Our observation that inter-tumor variability is the dominant source of variation in immune cell density in the tumor models evaluated suggests that animal-to-animal variability is a major contributor, likely arising due to the stochastic nature of tumor evolution which in turn impacts immune cell abundance.
- The relatively low intra-tumor variability that we observed for most of the biomarkers we evaluated suggests that a single tumor section is typically adequate to quantify immune cell abundance.
- The robust agreement between the CV values from the retrospective analysis of IHC-DIA data and the tumor samples analyzed in this study suggests that the small group size (n = 4 or 5 tumors/model) was adequate to recapitulate the inter-tumor variability that was observed from a large aggregate of data pooled from several studies.
- The strong correlation that we observed between the two DIA endpoints (i.e., cell density and stain area%) for all the biomarkers suggest that either of these endpoints can be used to assess immune cell abundance in murine tumors.

Conclusions

This study provides a comprehensive analysis of immunologic heterogeneity in murine tumor models. We anticipate that these results will provide guidelines for designing preclinical studies for drug discovery and development.

All procedures performed on animals were in accordance with regulations and established guidelines and were reviewed and approved by Pfizer's Institutional Animal Care and Use Committee.